High-temperature positron diffusion in Si, GaAs, and Ge

E. Soininen, J. Mäkinen, D. Beyer, and P. Hautojärvi
Helsinki University of Technology, Laboratory of Physics, 02150 Espoo, Finland
(Received 30 March 1992; revised manuscript received 30 June 1992)

Positron diffusion coefficients have been determined in Si, GaAs, and Ge in the temperature range 130–1000 K using the positron-beam technique. The diffusion coefficients at 300 K in Si, GaAs, and Ge are 2.3(2), 1.6(2), and 1–2 cm^2/s, respectively. In Si, the diffusion coefficient has the temperature dependence $T^{-1/2}$ from 30 to 500 K [combined with the experiment of Mäkinen *et al.*, Phys. Rev. B **43**, 12 114 (1991)], consistent with positron scattering from longitudinal acoustic phonons. At $T>500$ K the diffusion coefficients are lower than extrapolated from the $T^{-1/2}$ dependence indicating the onset of optical-phonon scattering. The first-order optical deformation-potential parameter is estimated to be 11 eV. Positron scattering from ionized impurities is observed in heavily doped *n*-type Si. In Ge, the temperature dependence of the diffusion coefficient is $T^{-1/2}$ above 500 K. At room temperature the experiment yields an abnormally high diffusion length which is attributed to space-charge effects. In GaAs the diffusion coefficient is only weakly dependent on temperature from 300 to 800 K, which is interpreted to be due to positron scattering from both acoustic- and polar-optical-phonon modes. The agreement with theory is good using the theoretical deformation-potential parameters and the positron effective masses $m^*=1.3m_e-1.6m_e$ in Si, GaAs, and Ge.

I. INTRODUCTION

Electron and hole mobilities in semiconductors are normally measured by application of the Hall effect or by the time-of-flight technique.[1-5] The carrier mobilities are well established in common semiconductors. The interactions with phonons and impurities provide the most important scattering mechanisms which limit the carrier mobilities. Phonon scattering also gives the dominating energy- and momentum-loss mechanism limiting the carrier drift velocity in high electric fields.

A positron exhibits transport properties similar to those of electrons and holes. The interest in positron motion and positron interactions with solids stems from various applications of the positron annihilation technique. On the other hand, the study of positron motion in semiconductors can improve the understanding of the microscopic processes limiting the carrier mobilities. The thermalized positron wave vector in solids is practically zero. The positron has a simple free-particlelike band structure in common semiconductors which facilitates the interpretation of experimental results. The application of the low-energy positron-beam technique also makes it possible to extend measurements to high temperatures, beyond those normally attainable by the current techniques for electrons and holes.[6]

The positron has an effective mass $m^*=1.3m_e-1.6m_e$, where m_e is the free-electron mass.[7] The heavy effective mass indicates relatively strong coupling to the lattice and consequently the diffusion coefficients and mobilities for positrons are lower than for electrons or holes. At 300 K, a calculation based on the positron band structure and acoustic-phonon scattering gives for the positron diffusion coefficient 2–3 cm^2/s in Ge and Si.[8] This corresponds to the positron diffusion length of ~ 0.2 μm and the mobility of ~ 100 $cm^2/V\,s$. The hole mobilities in Ge, Si, and GaAs at 300 K vary from 300 to 3000 $cm^2/V\,s$ and the electron mobilities from 1500 to 8000 $cm^2/V\,s$.[1,9-11] Besides the smaller positron mobility, the relative rates of various scattering processes change because of the large positron effective mass.

Positron annihilation has a variety of applications in solid-state research. The most utilized property of the positron is trapping by vacancies which has a clearcut effect on the annihilation characteristics.[12] In semiconductors, the positron-beam technique has been applied to studies of defects due to ion implantation,[13-18] defect structures in overlayers,[19,20] and interfaces.[21-24] The quantitative analysis in all these examples relies on the knowledge of positron motion. The aspirations to increased efficiency in slow positron production and brightness enhancement, e.g., by application of field-assisted moderators, can also benefit from improved understanding of positron motion in semiconductors.[25-27]

The study of positron motion in semiconductors began with the drift-velocity measurements based on the Doppler shift of the annihilation radiation in Ge and Si γ-ray detectors.[28,29] Recently, a similar experiment has been carried out in GaAs.[30] The drift of positrons to a biased metal-semiconductor interface has been studied by observing shifts in the fast positron implantation profile[31] or by application of the positron lifetime technique.[32]

In most positron-beam experiments the diffusion coefficients have been extracted from a 1–2-μm layer below the surface. In Si and Ge the early experiments gave positron diffusion coefficients which varied significantly.[19,21,33-36] Space-charge effects at semiconductors surfaces have been suggested to explain some of these anomalies.[19,26,34] Recent experiments for Au-Si surface barrier diodes under controlled electric field show

 ©1992 The American Physical Society

that, from 30 to 300 K, the diffusion coefficient in Si varies with temperature as $T^{-1/2}$.[37] This temperature dependence is consistent with positron scattering off longitudinal acoustic phonons. The recent experiments indicate that the diffusion coefficient at 300 K in Si is 2.6–3.1 cm^2/s.[19,32,37,38] In GaAs diffusion coefficients around 1 cm^2/s have been reported.[39,40]

In this paper we present the results of a positron-beam study of positron diffusion in Si, Ge, and GaAs in the temperature range 130–1000 K. The primary purpose of the study was to determine the positron diffusion coefficients at temperatures higher than 300 K where the experimental data is controversial and scarce to date. It is possible to identify the positron lattice-scattering mechanisms from the experimental data. Positron coupling to longitudinal acoustic phonons is the dominating lattice-scattering mechanism. In Si, positrons are also coupled to longitudinal optical phonons at temperatures higher than 500 K. An estimate $\Xi_1 = 11$ eV for the deformation-potential parameter for the first-order optical-phonon scattering is extracted from the data. In GaAs longitudinal polar-optical phonons have a significant contribution which is approximately equal to acoustic-phonon scattering. In heavily doped Si positron diffusion coefficients are 0.4–0.7 cm^2/s from 300 to 800 K, indicating scattering from ionized impurities. The agreement with theory is good using the theoretical deformation potentials for positron coupling to acoustic phonons and the positron effective masses $m^* = 1.3 - 1.6 m_e$. In Ge the experiment yields an abnormally high diffusion length at room temperature which is attributed to space-charge effects.

We outline the principle of the positron-beam technique in Sec. II. The experimental conditions are described in Sec. III. The analysis of positron-beam data is detailed and the measured diffusion parameters are presented in Sec. IV. In Sec. V we consider the influence of the space-charge effects on the positron data and compare the present results with other studies. The experimental diffusion coefficients are compared with calculations based on the elementary Boltzman transport theory in Sec. VI. This allows us to identify the various lattice- and impurity scattering processes. A summary of the results and conclusions will be given in Sec. VII.

II. POSITRON-BEAM TECHNIQUE

The measurement of an electron or a hole mobility requires an external electric field. In this study an attempt is made to observe field-free positron diffusion and we feel it is appropriate to focus on positron diffusion coefficients rather than mobilities. As thermal positron propagation in solids is described by random-walk motion, the positron diffusion coefficient D_+ can be related to the mobility μ_+ by the Einstein relation $D_+ = k_B T \mu_+ / e$, where k_B is the Boltzmann constant, T is the temperature, and e is the elementary charge.

Using the positron-beam technique, consistent results were obtained for positron diffusion in a number of cubic metals in a wide temperature range.[41] In agreement with theory, the diffusion coefficient varies with temperature as $T^{-1/2}$ which is characteristic of longitudinal acoustic-phonon scattering. The positron-beam technique has been discussed in detail elsewhere[42,43] and is only briefly presented here.

The study of positron diffusion with a low-energy positron beam involves positron motion to a surface. In the experiment, positrons are implanted into a solid where they rapidly (<10 ps) thermalize. The region where electron-positron annihilation takes place depends on the depth of implantation and the subsequent positron motion. Positrons may annihilate in the bulk or diffuse to the solid surface and annihilate there. Thereby the annihilation characteristics vary with the probability of back diffusion and with the incident energy of the positron. A study of this variation provides a direct way to determine the distance positron travels within its lifetime.

Positron annihilation at various incident energies is studied by recording the Doppler broadening of the annihilation line or the positronium (Ps) formation at the surface. The annihilation line-shape parameter S is defined as the ratio of counts in the central part of the 511-keV annihilation line to the total number of counts in the annihilation peak. For the incident positron energy E, let $J(E)$ be the probability of the positron to reach the surface of the sample prior to annihilation. Then the line-shape parameter $S(E)$ is a superposition of the characteristic value S_b of annihilation in the bulk and the value S_{surf} for annihilation at the surface region,

$$S(E) = S_{surf} J(E) + [1 - J(E)] S_b \ . \quad (1)$$

At clean surfaces positrons form positronium atoms with electrons at the surface. The fraction of positrons forming Ps atoms $f_{Ps}(E)$ is related to $J(E)$ by

$$f_{Ps} = f_{Ps}^0 J(E) \ , \quad (2)$$

where f_{Ps}^0 denotes the probability for a thermal positrons to form Ps at the surface. Positronium-formation measurements thus provide an alternative way to obtain information about positron bulk diffusion.

The main task in the data reduction is to separate the contributions of positron implantation and diffusion from the experimental back-diffusion probability $J(E)$. This transport problem has been treated starting from the classical carrier-transport models based on the drift-diffusion approximation. The quasistationary drift-diffusion equation reads as

$$D_+ \nabla^2 n_+(\mathbf{r}) - \lambda n_+(\mathbf{r}) - \nabla \cdot [n_+(\mathbf{r}) \mathbf{v}_d] + P(\mathbf{r}, E) = 0 \ , \quad (3)$$

where D_+ is the positron diffusion coefficient, $n_+(\mathbf{r})$ is the density distribution of thermal positrons, λ is the annihilation rate, and $\mathbf{v}_d$ is the positron drift velocity in an electric field. The positron implantation profile $P(\mathbf{r}, E)$ is the initial positron distribution after slowing down to thermal energies. The use of the diffusion model is limited to positrons which have been implanted deeper than several scattering mean free paths. It is also required that the scattering events are isotropic and quasielastic. At high temperatures relevant in this study and in the incident positron-energy ranges used for the analysis these

requirements are satisfied.[44,45]

The implantation profile can be expressed as[46]

$$P(z,E)=-\frac{d}{dz}\exp[-(z/z_0)^m] , \quad (4)$$

where z denotes the distance from the surface. The parameter z_0 is a function of the incident positron energy, given by $z_0=z_{1/2}/(\ln 2)^{1/m}$, and the median penetration depth of positrons is

$$z_{1/2}=A_{1/2}[E/\text{keV}]^n . \quad (5)$$

The choice of the implantation profile parameters m, n, and $A_{1/2}$ for Si, Ge, and GaAs is based on the Monte Carlo simulation of positron slowing down and it is discussed in Sec. IV A.

We use the drift-diffusion model to describe positron transport and to find the positron diffusion coefficient. In the analyses we also assume that the electric-field intensities are sufficiently small not to influence positron motion (see Sec. V). This simplifies the data analysis considerably. The surface boundary condition for the diffusion equation is $D_+(\partial n_+/\partial z)=\nu n_+$, where ν is the total escape rate at the surface. From Eq. (3), the probability of back diffusion and escape from the bulk is[47]

$$J(E)=\frac{\nu}{\nu+\frac{L_+}{\tau}}\int_0^\infty P(z,E)\exp[-z/L_+]dz . \quad (6)$$

The diffusion length is defined as $L_+=(D_+\tau)^{1/2}$ and τ is the positron lifetime. We have assumed a totally absorbing surface, $\nu \gg L_+/\tau$. The transition rate ν appears in Eq. (6) as a prefactor only and it has no effect on the diffusion parameters. By using the implantation profile of Eq. (4) the back-diffusion probability is expressed as

$$J(E)=-\int_0^\infty \exp[-z/L_+]\frac{d}{dz}\exp[-(z/z_0)^m]dz$$
$$=F_m(z_0/L_+) , \quad (7)$$

where the Laplace transform of the implantation profile with the shape parameter m has been denoted as F_m. As the implantation depth z_0 depends on the incident energy as E^n, it is customary to define a diffusion-related parameter E_0 through the equations

$$z_0=A_0E^n ,$$
$$L_+=\sqrt{D_+\tau}=A_0E_0^n , \quad (8)$$

where E and E_0 are expressed in keV. The relation between z_0 and $z_{1/2}$ yields $A_0=A_{1/2}/(\ln 2)^{1/m}$. The ratio $z_0/L_+=(E/E_0)^n$, and Eq. (7) can be written in the form

$$J(E)=F_m([E/E_0]^n) . \quad (9)$$

Thus for a known implantation profile (m and n given) the energy dependence of the back-diffusion probability $J(E)$ can be described by a single parameter E_0. The value of E_0 gives the diffusion length L_+ and the diffusion coefficient D_+ via Eq. (8).

It is important to notice from Eq. (8) that the back-diffusion probability $J(E)$ gives only the ratio of the implantation depth z_0 to the positron diffusion length L_+. Therefore any systematic error in the implantation depth is reflected in the absolute levels of L_+ and D_+ via Eq. (8). The temperature dependence of D_+ is, however, rather independent of uncertainties in z_0 (Sec. IV).

The main sources of systematical error in the analysis of positron diffusion data come from incomplete thermalization of positrons at small incident energies, from the positron implantation profile and from electric-field effects at semiconductor surfaces. In addition, positron trapping reduces the diffusion length, and would lead to a wrong interpretation of the diffusion coefficient. These aspects will be considered in more detail in Secs. III–V.

III. EXPERIMENT

A. Positron beam

The measurements were performed with a magnetically guided positron beam described in detail in Ref. 48. Positrons are produced in an encapsulated 100 mCi ^{22}Na source and moderated in a 7000-Å-thick single crystal W(100) foil in transmission geometry. The intensity of the positron beam at the target was typically $8\times10^5 e^+/\text{s}$, and the beam diameter was 4 mm. The incident positron energy was varied from 100 eV to 30 keV. The pressure in the unbaked vacuum chamber was 10^{-8}–10^{-7} mbar.

The annihilation spectra were detected and recorded with a high-purity Ge detector and a digitally stabilized multichannel analyzer system. The resolution corresponding to the measurement configuration and count rate measured with a ^{207}Bi source (570 keV) was 1.7-keV full width at half maximum (FWHM). In this study, the line-shape parameter S and the Ps yield f_{Ps} were extracted with standard methods from the annihilation γ-ray spectra.[42] The S parameter was defined as the ratio of counts in the 511.0 ± 0.9 keV peak region to the total number of counts in the annihilation peak 511 ± 7.3 keV. The Ps yield was calculated from the total spectrum, considering the number of counts in the annihilation peak containing the Ps 2γ annihilations and the counts in the region below the annihilation peak characterizing the Ps 3γ events. To measure the S parameter, more than 10^6 counts were collected to the annihilation peak at each incident positron energy. During the Ps yield measurements, more than 2×10^5 events were recorded.

Temperature was controlled with an electron-beam heater and measured with a type-K (NiCr/NiAl) thermocouple attached to the sample surface. To cool the sample below 300 K, a liquid-nitrogen cryostat was used. The accuracy of the temperatures is estimated to be better than ±5 K at 300 K and below. At high temperatures $T>800$ K the accuracy is typically ±20 K. The data at different temperatures were taken in random order unless otherwise stated.

B. Samples

For Si, Ge, and GaAs, there was a high-resistivity, intrinsic, and semi-insulating specimen, respectively. In addition, heavily doped Si and Ge were studied. In the

undoped samples the space-charge region extends so far that the electric field in the near surface layer becomes insignificant as long as there are no thermally generated charge carriers. At sufficiently high temperatures thermally generated charge carriers will effectively compensate the surface charge and it is difficult to support the field. In this study, both the cases of a very long (almost flat bands) and a very short band-bending region are confronted. The doped Si and Ge samples have a sufficiently high ionized impurity concentration for the band-bending region to be much shorter than the positron diffusion length.

The samples are listed in Table I. The resistivity of the high-purity floating-zone (FZ) refined Si was 10^4 Ω cm. The residual boron and phosphorus concentrations were 3.3×10^{12} and 1.4×10^{12} cm^{-3}. In semi-insulating 10^8-Ω cm liquid-encapsulated Czochralski (LEC) -grown GaAs the concentrations of C and Zn impurities are around 10^{15} cm^{-3}. The metal-organic vapor-phase epitaxially (MOVPE) grown GaAs sample (thickness 3.4 μm) is deposited on a GaAs(100) substrate and it is n-type with a carrier concentration 2×10^{14} cm^{-3}. The high-purity FZ Ge sample was cut from an intrinsic detector crystal. The doped samples were n-type Cz-Si, the resistivity of which is 8×10^{-4} Ω cm corresponding to the impurity concentration $[P]=10^{20}$ cm^{-3}, and n-type Ge($[As]=1.5\times10^{17}$ cm^{-3}).

We have no positron results on heavily doped GaAs due to inherent experimental difficulties. In strongly p-type GaAs an electric field is induced at the surface which prevents diffusing positrons from reaching the overlayer.[49] In an n-type specimen the field would be directed towards the surface (Sec. V). However, positron trapping to native vacancies has been observed in n-type bulk GaAs (Ref. 50) and therefore positron diffusion experiments in heavily doped n-type GaAs are distorted by positron trapping.

The surface orientations of the crystals are listed in Table I. The undoped specimen were polished with down to 0.25-μm diamond paste, etched to remove a 40-μm layer from the surface (for etches, see Table I), and mounted into the vacuum chamber. The n-type GaAs and the Ge(As) and Si(P) samples were measured as received by the supplier. For all samples no further surface treatment was made *in situ* unless otherwise stated later.

Positron lifetimes at 300 K in undoped Si, GaAs, and Ge are 217,[51] 231,[52] and 230 ps,[53] respectively (Table II). In the samples Si($[P]=10^{20}$ cm^{-3}) and Ge($[As]=1.5\times10^{17}$ cm^{-3}) the lifetimes at 300 K are 218 (Ref. 51) and 227 ps. These are all positron lifetimes in the bulk indicating that there is no trapping. In high resistivity Si positron trapping has not been detected at temperatures up to the melting point[53,54] and in Si($[P]=10^{20}$ cm^{-3}) up to 500 K.[51] Free positron lifetimes only have been observed in Ge up to the melting point[53] and in semi-insulating GaAs up to 600 K.[52] In all the experiments in this work positron diffusion is thus expected to be free from positron trapping at lattice defects.

We fabricated Schottky contacts on the high-purity and As-doped Ge samples. Ag and Cu layers of thicknesses 10–50 nm were evaporated on chemically

TABLE I. Characteristics and treatment of the Si, Ge, and GaAs samples. Samples were grown by the Czochralski (Cz), floating-zone (FZ), liquid-encapsulated Czochralski (LEC), or metal-organic vapor-phase epitaxy (MOVPE) method and provided by Centre d'Etudes Nucléaires de Grenoble (CEN), Centre National d'Electronique et Telecommunications (CNET), Laboratoire d'Electrotechnique, de Technologie et d'Instrumentation (LETI), Centre National de Research Scientifique in Valbonne (CNRS), Princeton Gamma-Tech (PGT), and University of California Lawrence Berkeley Laboratory (UCLBL).

	Si	Si(P)	GaAs Sample I	GaAs Sample II	Ge	Ge(As)
Doping concentration (cm^{-3})		10^{20}				1.5×10^{17}
Resistivity (Ω cm)	10^4	$<8\times10^{-4}$	10^8	4^a	47^b	3×10^{-2}
Impurity concentration (cm^{-3})	B 3.3×10^{12} P 1.4×10^{12} O,C $<10^{15}$		C,Zn 10^{15}–10^{16}		$3-5\times10^{10}$	
Conduction type	p	n	p	n	n	n
Growth method	FZ	Cz	LEC	MOVPE	FZ	FZ
Surface orientation		[111]	[100]	[100]		[111]
Supplier	CEN	CNET	LETI	CNRS	PGT	UCLBL
Etchant	HNO_3:HF CH_3COOH:H_2O 3:1:1:3		H_2SO_4:H_2O_2:H_2O 3:1:1		HNO_3:HF:H_2O 4:1:10	

[a] Calculated from the carrier concentration $n=2\times10^{14}$ cm^{-3}.
[b] Intrinsic resistivity (Ref. 1, p. 850).

TABLE II. Parameters used in the analysis of the positron diffusion data.

	Si	Si(P)	GaAs	Ge	Ge(As)
Positron lifetime					
τ (300 K) (ps)	217[a]	218[a]	231[b]	230[c]	227[d]
$\Delta\tau$ (ps/100 K)	0.6	1.3	0.6	0.3	
Energy range	3–23	3–22	sample I: 6–27	free surface: 3–26	4–29
in the analyses (keV)			sample II: 3–25	diodes: 6–29	4–29
Implantation profile parameters:					
Median penetration depth					
$A_{1/2}\rho$ (μg/cm^2)	2.7		3.5	3.5	
Density (g/cm^3)	2.33		5.32	5.33	
Parameter n	1.69		1.60	1.60	
Parameter m	1.9		1.8	1.8	

[a]Saarinen (Ref. 51).
[b]Lanki (Ref. 52).
[c]Würschum *et al.* (Ref. 53).
[d]Present work.

etched surfaces which were exposed to ambient pressure for a couple of minutes prior to the depositions. The metal overlayers were characterized by tunneling microscopy and photoelectron spectroscopy. The current-voltage characteristics were measured *in situ* in the positron experiment chamber to estimate the Schottky barrier heights. The diffusion coefficients were extracted from the measurements with flat-band voltages. However, there was large variation in the measured diode characteristics between different samples which indicates that the contacts were not always properly established. The diodes also showed pronounced aging effects. Metal-semiconductor contacts could not be used as an overall solution to control the electric fields due to interface reactions and interdiffusion between the metal and the semiconductor at evaluated temperatures.

IV. RESULTS

A. Positron implantation and data analysis

Figure 1(a) shows the S parameter as a function of the incident positron energy in Si at 130 and 900 K. In Fig. 1(b) similar data from high-resistivity Si and Si([P]$=10^{20}$ cm^{-3}) samples at 300 K are presented. In both samples at the given temperatures the effect of the electric field on positron motion can be neglected. The differences indicate a smaller positron diffusion length both at high temperatures and in the presence of a high concentration of ionized impurities. The changes in the absolute levels of the S parameter have no physical significance but are due to different measurement geometries for different samples.

Material-independent parameters $m \approx 2$, $n \approx 1.6$, and $A_{1/2} \approx (3.8\ \mu\text{g/cm}^2)/\rho$ have been used to characterize the positron implantation profile (ρ is the material densi-

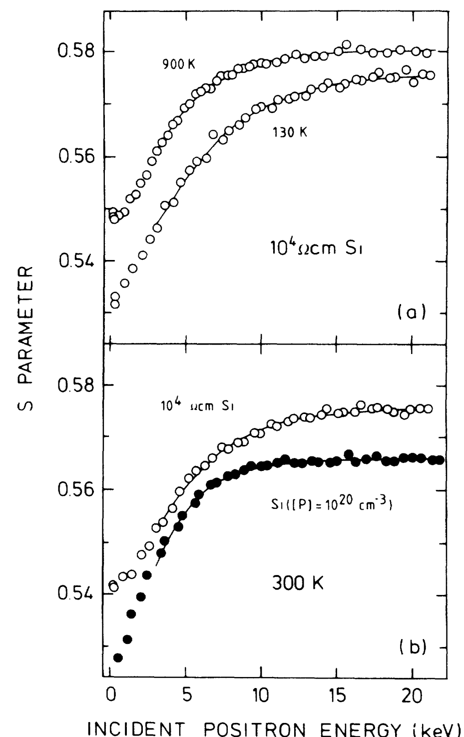

FIG. 1. The annihilation line-shape parameter S as a function of the incident positron energy in Si. In (a) the $S(E)$ curves are shown at 130 and 900 K. In (b) the results at 300 K from 10^4-Ω cm Si and Si([P]$=10^{20}$ cm^{-3}) are compared. The absolute level of the S parameter has been offset for the 900-K results in (a) for clarity. The changes in absolute levels of the S parameter are due to changes in the measurement geometry for different samples. The sample surfaces were covered by an oxide layer in all cases. The solid lines are fits to the diffusion model in the energy range 3–23 keV (see text).

ty).[46,55] Recently Baker *et al.*[56–58] have shown that the shape of the implantation profile is material dependent. To get reliable values for the parameters we have performed Monte Carlo simulations in the energy range 1–30 keV for Al, Si, Ge, and Au using the computer code of Valkealahti and Nieminen.[46] A fit of the median penetration depths of Eq. (5) as a function of the incident positron energy at $E > 3$ keV yields the parameters $A_{1/2}$ and n for each material. The parameters m were obtained by fitting the simulated implantation profile to Eq. (4). At the energy range 3–30-keV the parameters m, n, and $A_{1/2}$ were independent of the incident energy. The results of the fits for Al, Si, Ge, and Au are as follows: for Al,

$$m = 1.94(15)\ , \quad n = 1.69(5)\ ,$$
$$A_{1/2} = [2.8(5)\ \mu\text{g/cm}^2]/\rho\ ,$$

for Si,

$$m = 1.91(16)\ , \quad n = 1.69(2)\ ,$$
$$A_{1/2} = [2.7(2)\ \mu\text{g/cm}^2]/\rho\ ,$$

for Ge,

$$m = 1.78(8)\ , \quad n = 1.60(3)\ ,$$
$$A_{1/2} = [3.5(4)\ \mu\text{g/cm}^2]/\rho\ ,$$

and for Au,

$$m = 1.70(8)\ , \quad n = 1.48(3)\ ,$$
$$A_{1/2} = [6.0(5)\ \mu\text{g/cm}^2]/\rho\ .$$

In Al and Au the simulated implantation profiles are essentially the same as those obtained in recent experimental and Monte Carlo studies.[56–58] The simulated backscattering probabilities are in a very good agreement with the recent experimental results of Massoumi *et al.*[59] The simulated parameters for Al ($Z = 13$) are the same as for Si ($Z = 14$). For this reason we assume that the parameters for Ge ($Z = 32$) can be used for GaAs ($Z_{Ga} = 31$, $Z_{As} = 33$) as well. Even though there is no direct experimental evidence for the parameters in Si, Ge, or GaAs, the good agreement in other materials between these simulations, other independent simulations,[56,58] and experiments[56–59] gives credence to this choice. For Si we have chosen parameter values $m = 1.9$, $n = 1.69$, and $A_{1/2} = (2.7\ \mu\text{g/cm}^2)/\rho$. For Ge and GaAs the parameters are $m = 1.8$, $n = 1.60$, and $A_{1/2} = (3.5\ \mu\text{g/cm}^2)/\rho$. An implantation profile parameterization somewhat different from that of Eq. (4) has recently been suggested by Baker *et al.*[56] but we do not expect this to have any noticeable effect on the results.

The data were fitted with a method of least squares to the diffusion model using Eqs. (1) and (7) or (2) and (7). The free parameters in the fitting of the line-shape parameter $S(E)$ were S_{surf}, S_b and E_0 and in the fitting of the Ps fraction $f_{Ps}(E)$ they were f_{Ps}^0 and E_0. The analyzing programs are described in Ref. 43.

The surfaces were intentionally covered with thin oxide layers whenever possible. Line-shape parameter data $S(E)$ were used for Si and GaAs. The Ps fraction $f_{Ps}(E)$ was always measured simultaneously with $S(E)$. When a significant fraction of positrons form Ps at the surface [$f_{Ps}(E) > 10$–$20\,\%$], the linearity of Eq. (1) no longer holds.[43] In all Si and GaAs surfaces studied $f_{Ps}(E)$ was less than 10% at all temperatures in the energy range chosen for the analysis. The only exception was semi-insulating GaAs at the highest temperatures where $f_{Ps}(E)$ was still less than 20%. From Ge surfaces the oxide layer desorbs already below 700 K and for the high-purity Ge sample $f_{Ps}(E)$ data were used for the analysis.

In Fig. 1 the data have been fitted to the diffusion model in the energy range $E_{min} - 23$ keV. Low incident energies ($E_{min} = 3$–6 keV) are omitted in the analysis because at low energies (i) a significant fraction of the positrons returning to the surface are epithermal,[47,60–62] (ii) the implantation profile parametrization breaks down,[63] and (iii) in some cases the Ps production causes nonlinearities in Eq. (1).[43] The energy ranges used for the analyses are listed in Table II. The diffusion coefficients are within the statistical errors of the analysis if the cutoff in energy is from 1 to 5 keV in Si, from 1 to 4 keV in P-doped Si, and from 3 to 6 keV in GaAs (see Table III). The rather high cut-off energy (6 keV) in the case of the GaAs sample I was used to reduce the possible influence of Ps formation (see below). In Ge the cutoff in energy is rather high in some cases to be sure that the metal overlayers do not distort the positron data. In practice the cutoff in energy has almost no influence on the diffusion coefficients as long as it is within the limits given above.

B. Silicon

The experimental results for the positron diffusion coefficient D_+ in Si as a function of temperature from 130 to 1000 K are presented in Fig. 2(a). The results from two samples with different surface oxidations are shown. The diffusion coefficients measured from the doped Si([P] = 10^{20} cm^{-3}) sample from 300 to 800 K are also presented.

For reproducible results it was found necessary to have an oxide layer on the Si surface. One of the samples [open triangles in Fig. 2(a)] was exposed to ambient air for several months, which is known to produce a thin native oxide layer.[64] The other sample (open circles) was sputtered *in situ* with 500-eV Ar^+ ions at normal in-

TABLE III. The positron diffusion coefficient D_+ at 300 K. The errors are results of statistical analyses of the data.

	Si	Si([P] = 10^{20} cm^{-3})	GaAs	Ge	Ge([As] = 1.5×10^{17} cm^{-3})
D_+(300 K) (cm^2/s)	2.3(2)	0.45(6)	1.6(2)	0.9–2.1	0.84(9)

cidence at 10^{-4} mbar of Ar for 1 h (residual gas partial pressure was less than 10^{-5} mbar) and annealed at 1000 K at 2×10^{-7} Torr residual gas (CO, H_2O) pressure for 15 min. The formation of the oxide layer was confirmed by x-ray photoelectron spectroscopy (XPS). An XPS spectrum taken a few hours after etching the sample showed a few ångströms of oxygen on the surface but no signs of oxide formation. After the sputtering and annealing a 25-Å-thick layer of silicon oxide had formed on the surface.

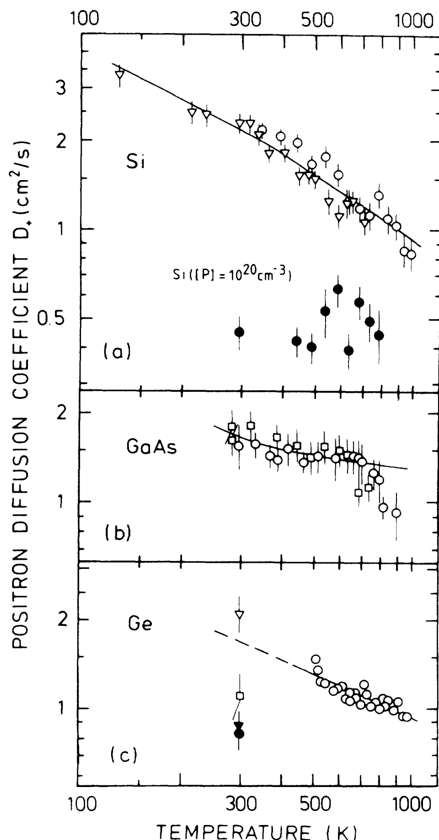

FIG. 2. The temperature dependence of the positron diffusion coefficient in Si, GaAs, and Ge. (a) Si. Results from two 10^4-Ω cm Si samples are shown as open circles and triangles. The solid circles are the diffusion results from the Si([P]$=10^{20}$ cm^{-3}) sample. All the Si surfaces were covered by an oxide layer. (b) GaAs. The circles and squares denote measurements from the LEC-grown semi-insulating and the MOVPE-grown $n=2\times10^{14}$ cm^{-3} GaAs sample, respectively. The GaAs surfaces were not intentionally cleaned *in situ*. (c) Ge. The open circles are results from the oxide-free Ge surface. The open triangle and the open square are the results of the diffusion measurements from the Cu-Ge and Ag-Ge Schottky diode, respectively. The diffusion coefficients in Ge([As]$=1.5\times10^{17}$ cm^{-3}) measured from the oxide- and Ag-covered surface are shown as a solid triangle and a solid circle, respectively. Except for the data at $T>500$ K in Ge [open spheres in (c)], the diffusion coefficients are based on the S parameter data. The curves through the data are theoretical calculations based on positron-phonon scattering (Sec. VI). The errors shown are due to statistical variations.

We introduce the parameter S_s/S_b which is defined as the ratio of the S parameter at the surface region to that in the bulk. The parameter S_b is obtained from a fit to Eq. (1) and S_s is the experimental value of the S parameter at $E=100$ eV. The ratio S_s/S_b can be used to characterize the state of the sample surface. In both Si samples the ratio S_s/S_b at 130–1000 K was 0.92–0.95. We take this as an indication for the existence of a surface oxide layer; the ratio is $S_{SiO_2}/S_{Si}=0.95$–0.97 in dry-oxidized SiO_2/Si structures.[24,65]

After having taken data from the sample with a native oxide at about 700 K, the positron experiment gave abnormally high values of S_s/S_b and low values of E_0 at lower temperatures. The results recovered within about one day back to the earlier values. High values of S_s/S_b and low values of E_0 were also extracted from the chemically etched surface as mounted. After the sputtering-heat treatment the oxide layer and the interface were stable and the positron results were reproducible between 300 and 1000 K. Such unexpected positron results may be associated with changes in the nature and distribution of interface or surface states (Sec. V). It can be concluded that when the ratio S_s/S_b is within the range of 0.92–0.95 the positron experiment gives consistent results for the positron diffusion parameters.

From Fig. 2(a) it is evident that the positron diffusion coefficient D_+ in silicon follows the power law $T^{-\alpha}$ in the temperature range 130–500 K. The diffusion coefficient at 300 K is $D_+=2.3(2)$ cm^2/s. In the temperature range 130–500 K a good fit to the power law $D_+=D_0(T/300\ \mathrm{K})^{-\alpha}$ is obtained yielding $\alpha=0.50$. Above 500 K, the values of D_+ are lower than those extrapolated from the low-temperature values assuming the same temperature dependence.

In the Si([P]$=10^{20}$ cm^{-3}) sample the positron diffusion coefficients are 0.4–0.7 cm^2/s from 300 to 800 K [Fig. 2(a)]. The data were taken in an increasing order of temperatures, and the ratio S_s/S_b changed from 0.93 at 300 K to 0.94 at 800 K.

At 900 K, the ratio S_s/S_b in Si([P]$=10^{20}$ cm^{-3}) increased to 0.96 due to increased surface parameter S_s. The diffusion coefficient dropped at 900 K and remained at a constant level 0.1–0.4 cm^2/s when cooling the sample down to 600 K (not shown). The parameter S_s/S_b returned back to 0.93 and S_s descended to its value before heating. Some irreversible change had occurred reducing positron diffusion but not affecting its annihilation line shape. This observation could be related to the dopant impurity redistribution during the annealing at 900 K.[64,66]

We have evaluated the effect of implantation profile parameters on the final results. The 300-K diffusion coefficient in Si fitted using the parameters $m=2$, $n=1.6$, and $A_{1/2}=(3.75\ \mu g/cm^2)/\rho$ is 3.0(2) cm^2/s. The implantation profile given by $m=1.9$, $n=1.69$, and $A_{1/2}=(2.7\ \mu g/cm^2)/\rho$ decreases the absolute values of the diffusion coefficient by 24% to 2.3(2) cm^2/s in Si, mainly due to the smaller median implantation depths $z_{1/2}=A_{1/2}E^n$. The decrease is the same at all temperatures, i.e., the implantation profiles yield the same tem-

perature dependence for the positron diffusion coefficient. The same effect is seen in Ge and GaAs.

C. Gallium arsenide

The positron diffusion coefficients D_+ in GaAs as a function of temperature from 300 to 900 K are shown in Fig. 2(b). The results were obtained from surfaces which were not intentionally cleaned *in situ*.

As mounted, the LEC-grown semi-insulating GaAs sample I gave an almost flat $S(E)$ curve, characterized by $S_s/S_b < 1.02$. The sample was annealed *in situ* at 620 K for several hours which resulted in a surface where the maximum positron fraction at a few hundred eV incident positron energies was 20%, and the ratio S_s/S_b was 1.04–1.09 from 300 to 770 K. At 870 K a sharp increase in the positronium formation was observed, indicating desorption of the surface oxide layer. This observation is in agreement with other studies.[67] Thereafter, at lower temperatures there was Ps formation up to 50% at the surface at low incident positron energies and the ratio S_s/S_b increased to 1.10–1.12. The lowest energies were omitted from the fits up to 6 keV because of the large Ps fraction (Sec. IV A). The diffusion results were not influenced by the change in the surface condition at 870 K.

The measurements from the MOVPE-grown GaAs sample II were performed in an increasing order of measurement temperatures. After each measurement at high temperature, data were taken near 300 K to monitor changes in the surface condition. The parameter S_s/S_b was 1.02–1.05 from 300 to 700 K both during the measurements at high temperatures and in the subsequent measurements at 300 K. At 750 K the Ps fraction increased strongly and the ratio S_s/S_b changed to 1.07. No more data were taken after the change in the surface condition. In both samples the bulk parameter S_b increased by less than 0.1%/100 K up to the highest measurement temperatures. This increase is consistent with lattice expansion.

The positron diffusion coefficient in GaAs at 300 K is $D_+ = 1.6(2)$ cm^2/s. From 300 to 800 K, the diffusion coefficient exhibits a weak temperature dependence being 1.4(1) cm^2/s at 700 K. At high temperatures $T \geq 800$ K, the diffusion coefficient decreases more rapidly.

D. Germanium

In Fig. 2(c) we present the results for the positron diffusion coefficient in high purity Ge. The results above 500 K are obtained from a free surface. The 300-K values are measured from Ag-Ge and Cu-Ge Schottky diodes. Also shown in Fig. 2(c) is the diffusion coefficient in Ge([As]$=1.5\times10^{17}$ cm^{-3}) at 300 K, measured from a free and an Ag-plated surface.

As mounted, the high-purity Ge sample yielded the S parameter ratio $S_s/S_b = 0.96$–0.97, practically no Ps formation, and the diffusion parameter E_0 from 5 to 6 keV at 300–500 K. The surface oxide layer desorbs easily from Ge at elevated temperatures, and the residual gases adsorb on the surface again at lower temperatures.[68] When heating the sample at 870 K for 10 min the Ps fraction increased to more than 50% at low energies at all temperatures indicating oxide desorption, and the surface to bulk ratio was $S_s/S_b \approx 1.11$. Strong Ps formation distorts the S parameter data (cf. Sec. IV A), and therefore the Ps fraction data were used in the analysis.

The diffusion parameters E_0 [cf. Eq. (8)] measured from the free annealed surface of the high-purity Ge sample are shown in Fig. 3 for the whole temperature range 300–970 K from six different sets of measurements. The values of E_0 above 500 K decrease slowly from 6.7 to 6.2 keV at 970 K. Below 500 K a steep rise is observed, and at 300 K $E_0 \approx 9.7$ keV.

Several Ag-Ge and Cu-Ge Schottky diodes were fabricated on the high-purity Ge sample in order to produce flat energy bands at the surface by biasing the diodes. The results shown in Figs. 2(c) and 3 were obtained from 20- and 50-nm Ag-Ge and from 20-nm Cu-Ge Schottky diodes. A correction to the implantation profile [Eq. (4)] was made to compensate for positron slowing down in the metal overlayer.[55] The E_0 values are 6.5(4) and 8.0(3), and the corresponding results for D_+ are 1.1(2) and 2.1(3) cm^2/s in the Ag-Ge and the Cu-Ge diode, respectively.

Both Ge Schottky diodes yield values of E_0 which are significantly smaller than at the free annealed Ge surface at 300 K. The diffusion coefficients, however, differ by a factor of 2 between Cu-Ge and Ag-Ge. It may be that the band flattening has not been completed. The diodes also showed pronounced aging effects.

The arguments in Sec. V suggest that below 500 K space charge near the surface distorts free positron diffusion. This is supported by the experimental results where the diffusion parameters from the Schottky diodes with almost flat bands are different from the results at free surfaces. Therefore, only the high-temperature part

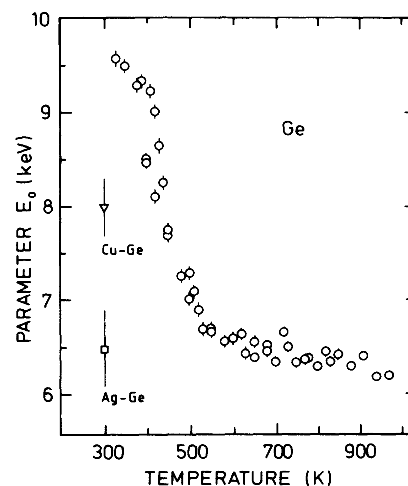

FIG. 3. The variation of the parameter E_0 with temperature in Ge. The circles are the results of several sets of measurements from the free Ge surface. For comparison, the parameters E_0 at 300 K for the flat-band biased Cu-Ge and Ag-Ge Schottky diodes are shown as a triangle and a square, respectively.

of the free-surface data is regarded representative of free diffusion and the results from temperatures below 500 K are not shown in Fig. 2(c).

The Ge([As]$=1.5\times10^{17}$ cm^{-3}) sample yields the parameter ratio $S_s/S_b\approx0.94$. The 300-K value of the diffusion coefficient in the Ge(As) sample, 0.82(9) cm^2/s, is a combination of several measurements from oxide-covered samples. The measurement from an etched and 10-nm Ag-plated sample gives $D_+=0.87(10)$ cm^2/s.

V. SPACE-CHARGE EFFECTS AND COMPARISON WITH OTHER EXPERIMENTS

One source of systematic error in the analysis of positron diffusion data is due to the electric-field effects at semiconductor surfaces. The drift length of positrons under an electric field is $l_+=\mu_+\mathcal{E}\tau$, where $\mathcal{E}$ is the electric-field intensity, μ_+ is the positron mobility, and τ is the positron lifetime. The electric field becomes effective when the drift length l_+ is of the order of the diffusion length L_+. As the positron lifetime is typically $\tau\approx220$ ps and the positron diffusion coefficient $D_+\approx2$ cm^2/s which corresponds to $\mu_+\approx80$ cm^2/V s and $L_+\approx0.2$ μm, the condition $l_+\approx L_+$ is reached when the electric field is approximately 1 kV/cm. Electric fields larger than 1 kV/cm arise at free semiconductor surfaces due to a distribution of charges near the surface. In the following we discuss the space-charge effects and compare the results with other experiments.

The positron diffusion coefficient in Si at 300 K is $D_+=2.3(2)$ cm^2/s. The diffusion coefficient 2.6–3.0 cm^2/s has been reported in recent bulk[32] and beam studies[19,34,37,38] in Si. Somewhat lower values were obtained in earlier experiments.[21,29,33] Below 300 K, three experiments have been reported.[29,32,37] In a positron-beam study on positron mobility in Au-Si diodes, the diffusion coefficient was found to follow the temperature dependence $T^{-1/2}$ from 30 to 300 K.[37] Those experimental results, reanalyzed using the implantation profile parameters given in Table II, are shown in Fig. 4 (Sec. VI A) for $T\geq80$ K for comparison. These two experiments yield the same diffusion coefficient. The bulk studies[29,32] are qualitatively in line with the beam experiments. Thus there is a good agreement between the present and recent experiments at $T\leq300$ K.

At free semiconductor surfaces the band-bending potential is determined by the position of the Fermi level at the surface, set by the balance of the surface charge and the induced subsurface electric field.[69] In intrinsic semiconductors, the overall charge neutrality is achieved through accumulation of free charge carriers near the surface.[70] At cleaved Si surfaces, the Fermi-level pinning position has been measured to be 0.3 eV above the valence-band edge[71] which coincides with a peak in the SiO_2-Si interface state density at 0.3–0.4 eV.[72] Assuming the typical Fermi-level position one-third of the band gap above the valence-band edge, the distance from the valence band is approximately $15k_BT$ at 300 K. The free-carrier concentration is small, and the subsurface electric-field intensity is less than 1 kV/cm. We thus expect that the positron diffusion coefficient is free of any charge effects in 10^4 Ω cm Si. The same conclusion can be made if one compares the result with the experiments on gold-plated Si Schottky diodes which yield the same diffusion coefficient.

Before the present results there was no consistent experimental data available on positron diffusion in Si at temperatures higher than 300 K. We observe the diffusion coefficient to decrease more rapidly than $T^{-1/2}$ above room temperature. This effect is clearly seen in the temperature range $T\geq500$ K. At the highest temperatures $T>800$ K the accumulated free-carrier concentration near the surface in Si becomes very high if there is any band bending. Numerical solution of the Poisson equation assuming the total band bending 0.1–0.2 eV asserts that the carrier concentration is sufficient for the electric field to be confined close (<500 Å) to the surface compared with the positron diffusion length. Thereby the observed positron motion is practically field free. This indicates that the decrease in the diffusion coefficient from 300 to 1000 K is not due to the subsurface electric field.

In the heavily doped Si(P) samples the carrier concentration is approximately 10^{20} cm^{-3}. The electric field, although it may have a very high intensity, goes to zero at a distance (<200 Å) which is much smaller than the positron diffusion length. As shown in Sec. VI, the ionized impurity scattering qualitatively accounts for the small diffusion coefficient 0.4–0.7 cm^2/s.

In GaAs, the positron diffusion coefficient at 300 K is $D_+=1.6(2)$ cm^2/s. The diffusion coefficient in GaAs at room temperature has been reported to be 0.9–2.1 cm^2/s.[30,39,40] Although there is some scatter in the reported values, the agreement with the present experiment is good.

At oxidized GaAs surfaces, the experimentally measured position of the Fermi level lies 0.4–0.55 eV and 0.7–0.9 eV above the maximum of the valence band in p- and n-type samples, respectively.[73] As the Fermi level usually pins close to midgap, it is so far from the valence- (and conduction-) band edges that no substantial hole (or electron) accumulation occurs at 300 K. Also the total band bending in semi-insulating GaAs is small. Therefore the electric field in semi-insulating GaAs is expected to be small, and the positron diffusion experiment is not influenced by electric-field effects below 500 K.

At high temperatures the arguments are more indirect as the intensity of the subsurface field depends on the detailed position of the Fermi level at the surface. The MOVPE grown GaAs sample which is n-type ($n=2\times10^{14}$ cm^{-3}) yields the same positron diffusion coefficient as the semi-insulating sample from 300 to 700 K. We also measured the positron diffusion coefficient in Te-doped ($n=2\times10^{15}$ cm^{-3}) MOVPE-grown GaAs at room temperature. The diffusion coefficient $D_+=1.7(2)$ cm^2/s is the same as in the other GaAs samples. Equal positron diffusion coefficients in semi-insulating and n-type GaAs samples strongly suggests that the experimental values of the diffusion coefficient are not distorted by space-charge effects.

Positron diffusion parameter values $E_0=6$–7 keV were found in a positron-beam experiment on n-type

($n=2.5\times10^{14}$ cm^{-3} and $n=2.2\times10^{16}$ cm^{-3}) undoped GaAs samples in the temperature range 300–700 K.[39] Using the present implantation profile these results correspond to $D_+=0.9-1.5$ cm^2/s, and the diffusion coefficient is independent of temperature. The result agrees with the present experiment supporting the observation that the diffusion coefficient depends very weakly on temperature in this temperature range.

At chemically etched oxide-covered Ge surfaces the Fermi-level position 0.13 eV above the valence-band edge has been reported.[74] However, since at most covalent semiconductor surfaces the peak density of surface states lies at approximately one-third of the band gap above the valence-band edge, it has been argued that this could be the Fermi-level pinning position at free Ge surfaces as well.[1] In Ge the band gap is $E_g=0.66$ eV at 300 K and the energy difference between the Fermi level and the valence-band edge at surface is so small that major accumulation of holes occurs already at room temperature if there is any band bending at the surface. If the total band bending is 0.1 eV in intrinsic Ge, the hole accumulation leads to an electric field which severely affects the positron motion. At 500–600 K the accumulated hole concentration becomes sufficient to screen the surface charge at the distance which is small compared with the positron diffusion length.

The experimental results in Ge are in accordance with this picture of electric field at the surface. Abnormally large diffusion parameters of $E_0\approx10$ keV were measured from the free Ge surface near 300 K. Above 500 K the parameter E_0 and its temperature dependence are quite similar to those observed in Si, leading to the positron diffusion coefficient ~1 cm^2/s and the temperature dependence which is close to $T^{-1/2}$. The diffusion parameters E_0 from the flat-band biased Schottky diodes and from the As-doped sample were 6–8 keV at 300 K, as expected from the high-temperature results. It seems evident that the free-surface results are affected by strong electric fields below 500 K.

The only measurements of positron motion in Ge above 300 K were made by Jorch *et al.*[35,36] In that positron-beam study very low diffusion coefficients were reported. The temperature dependence of the parameter E_0 reported by Jorch *et al.* closely resembles that presented in Fig. 3, particularly for the Ge(110) surface. As discussed above, we anticipate that the temperature dependence is due to space-charge effects which severely interfere with the positron experiment because of the small band gap in Ge.

VI. POSITRON-SCATTERING MECHANISMS

In Sec. IV the experimental results on the positron diffusion coefficient in the temperature range 130–1000 K in Si, GaAs, and Ge were presented. In this section we relate the experimental diffusion coefficients to the scattering mechanisms.

The scattering processes which are considered are due to long-wavelength longitudinal phonons and ionized impurities. Positron interaction with phonons is expected to be weak which means that the lattice distortion around a positron is small and lowest-order perturbation theory gives a good description of the positron motion.[45] This picture is consistent with the relatively large diffusion coefficient $D_+\geq1$ cm^2/s up to 1000 K.

In Si and Ge, lattice scattering due to nonpolar-acoustic and -optical phonons is included. In the lowest order, selection rules allow positron scattering from the acoustic modes only. We have modeled the experimental data in Si including the first-order optical-phonon scattering, i.e., the positron coupling to optical phonons in which the interaction is of the first order in the phonon wave vector. Even though the inclusion of this mechanism is not critical in explaining the temperature dependence of positron diffusion, it very much improves the agreement with the experiment at $T>500$ K. In Ge the data are insufficient to make conclusions about the contribution of optical phonons. In GaAs coupling to polar-optical and -acoustic phonons is considered. In particular, the polar-optical phonon scattering is important in explaining positron diffusion in GaAs.

The identification of the scattering processes is greatly facilitated by the simple positron band structure which is free-particlelike with a minimum at the Γ point.[8,75] Only one band needs to be considered, and complications due to interband scattering or carriers in multiple bands are avoided. The parabolic, spherically symmetric band minimum makes the calculations straightforward. Another special feature of the positron is its heavy effective mass, $m^*=1.3-1.6m_e$.[7] This is the primary reason for the low positron diffusion coefficients but it also greatly changes the relative rates of the various scattering processes in comparison with electrons and holes.

Apart from the polar-optical-phonon scattering, the scattering processes are treated in the relaxation-time approximation. The diffusion coefficient D_+ is calculated from the Einstein relation where the mobility is given by elementary transport theory as[76,77]

$$\mu_+=\frac{2e}{3m^*p}\int dE_k\rho(E_k)E_k\tau(E_k)\left[-\frac{\partial f_0}{\partial E_k}\right]. \quad (10)$$

Here p is the positron density, $\tau(E_k)$ is the momentum relaxation time for a positron of energy E_k, $\rho(E_k)$ is the density of states, and f_0 is the distribution function. For calculation of the average in Eq. (10) Maxwell-Boltzmann statistics and parabolic bands were used. The total relaxation time due to different scattering processes is assumed to have the form

$$\frac{1}{\tau(E_k)}=\sum\frac{1}{\tau_i(E_k)} . \quad (11)$$

We now treat the positron-scattering processes in Si, GaAs, and Ge separately. When available, theoretical coupling constants have been used. Since no firm values exist for the positron effective mass m^*, it has been used as an adjustable parameter.

A. Silicon

The lattice-scattering processes considered for Si are due to acoustic- and nonpolar-optical-phonons. Positron

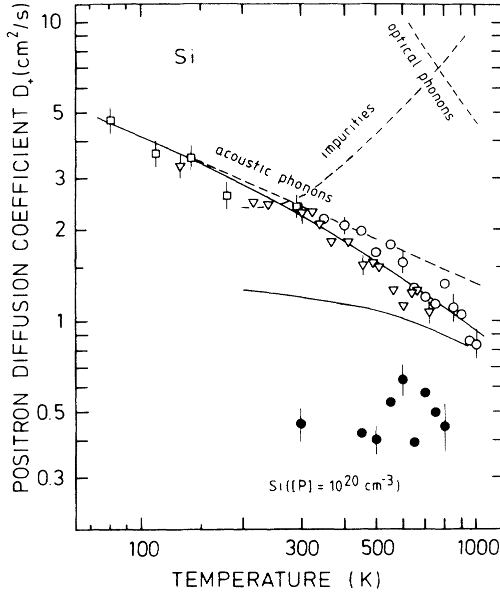

FIG. 4. Positron-scattering mechanisms in Si. The experimental data are reproduced from Fig. 2(a). The squares are diffusion coefficients from the measurements of Mäkinen *et al.* (Ref. 37) from biased Au-Si Schottky diodes reanalyzed using the present implantation profile parameters. The dashed lines represent positron diffusion coefficients due to scattering of acoustic and optical phonons and ionized impurities (see text and Table IV). The upper solid curve is obtained by combining the contributions of the two phonon modes. The combined diffusion coefficients due to lattice and impurity scattering are shown in the lower solid curve.

interaction with long-wavelength longitudinal acoustic (LA) phonons is treated using the deformation-potential approximation. The momentum relaxation time is given by[9,10]

$$\tau_{\mathrm{LA}}=\frac{\pi}{\sqrt{2}}\frac{\hbar^4 c_L}{E_d^2 m^{*3/2} k_B T E_k^{1/2}} \tag{12}$$

and the parameters used in the calculations are listed in Table IV. According to the band-structure calculation, the positron deformation-potential parameter in Si is $E_d=-6.19$ eV.[8] In Eq. (12) c_L is the average elastic constant for longitudinal phonons modes.

The deformation-potential approximation for the acoustic-phonon scattering gives the temperature dependence $D_{\mathrm{LA}} \propto T^{-1/2}$ for the diffusion coefficient. This temperature dependence is found for the diffusion coefficients up to about 500 K [Fig. 2(a)], indicating that positron motion in Si is determined by scattering off longitudinal acoustic phonons in the temperature range 130–500 K. We have combined the present results with those of Mäkinen *et al.*[37] at 30–300 K in Fig. 4. It can be concluded that positron coupling to longitudinal acoustic phonons limits positron diffusion in Si from 30 to 500 K, and that it is the most important scattering process up to 1000 K. The results for the diffusion coefficient due to acoustic phonons D_{LA} shown in Fig. 4 were calculated using $m^*=1.6m_e$, which yields the best agreement with the experiment (see below).

The deviation of the experimental diffusion coefficients from the temperature dependence $D_{\mathrm{LA}} \sim T^{-1/2}$ above 500 K is not due to positron trapping (Sec. III B) or electric fields (Sec. V). Another scattering process must set on at elevated temperatures. We have considered positron interactions with nonpolar-optical phonons using the deformation-potential approach. Due to the symmetry restrictions, the zeroth-order optical deformation-potential parameter for intraband scattering vanishes for an s-like band minimum at Γ point.[10] This is the case with positrons in Si (also in Ge and GaAs). On the other hand, first-order optical-phonon processes, proportional to the differential displacements within the unit cells, are still possible. A deformation-potential parameter Ξ_1 analogous to acoustic phonons can be defined. The momentum relaxation time for the first-order processes has been derived by Ridley[10] and it is given by

$$\tau_{\mathrm{LO}}=\frac{4\pi\rho\hbar^5\omega}{\Xi_1^2(2m^*)^{5/2}E_k}\{n(\omega)(E_k+\hbar\omega)^{1/2}[\tfrac{8}{3}+\tfrac{5}{3}(\hbar\omega/E_k)]+\theta(E_k-\hbar\omega)[n(\omega)+1](E_k-\hbar\omega)^{1/2}[\tfrac{8}{3}-\tfrac{5}{3}(\hbar\omega/E_k)]\}^{-1} . \tag{13}$$

TABLE IV. Material parameters for Si. These values were used to calculate the positron diffusion coefficient due to positron interactions with acoustic and optical phonons [Eqs. (12) and (13)] and ionized impurities [Eq. (14)]. Key to parameters: E_d, deformation-potential parameter; c_L, average elastic constant for longitudinal phonon modes; m^*, positron effective mass (m_e, free-electron mass); $\hbar\omega$, optical-phonon energy in a long-wavelength limit; Ξ_1, first-order optical deformation-potential parameter; N_D, impurity concentration; ε_r, dielectric constant.

E_d (eV)	c_L (N/m^2)	m^*	$\hbar\omega$ (meV)	Ξ_1 (eV)	N_D (cm^{-3})	ε_r
-6.19^a	18.9×10^b	$1.6m_e$	64^c	6.0	10^{20}	11.9^c

[a]Boev, Puska, and Nieminen (Ref. 8).
[b]The average was calculated as $c_L=c_{12}+2c_{44}+\frac{3}{5}(c_{11}-c_{12}-2c_{44})$ (Ref. 10). Data from Ref. 11.
[c]Reference 11.

The long-wavelength optical-phonon energy in Si is $\hbar\omega = 64$ meV,[11] and $n(\omega)$ is the phonon number given by the Bose-Einstein distribution.

The calculated diffusion coefficients $D_{\rm LO}$ due to first-order optical-phonon scattering in Si are shown in Fig. 4. The optical deformation-potential parameter Ξ_1 was adjusted as there is no theoretical value. The diffusion coefficient approximately follows the power law $D_{\rm LO} \propto T^{-3/2}$. By combining the scattering rates due to acoustic and optical phonons via Eq. (11), the upper solid curve in Fig. 4 is obtained for the positron diffusion coefficient. The inclusion of optical phonons has the effect of lowering the diffusion coefficient at high temperatures. A very good agreement with the experimental data was reached by adjusting the two parameters m^* and Ξ_1. The best fit was obtained with the positron effective mass $m^* = 1.6 m_e$ and the deformation-potential parameter $\Xi_1 = 11$ eV.

The values of the effective positron mass $m^* = 1.6 m_e$ is in agreement with other theoretical and experimental estimates. The values usually obtained for m^* lie between $1.3-1.6 m_e$.[7,8] The inclusion of first-order optical-phonon scattering with $\Xi_1 = 11$ eV yields a good fit to the experimental results. First-order processes have been used to explain electron mobility in Si. The deformation potential for electrons in Si is 5.6 eV.[78]

The phosphorus doping $[{\rm P}] = 10^{20}$ cm^{-3} of Si reduces the positron diffusion coefficients to $D_+ = 0.4-0.7$ cm^2/s from 300 to 800 K [Figs. 2(a) and 4]. We have estimated the effect of impurity scattering by using the Brooks-Herring model of the ionized-impurity scattering. The relaxation time is given by[9,10]

$$\tau_{ii} = \frac{1}{\pi N_i} \left[\frac{4\pi\varepsilon_0\varepsilon_r}{e^2} \right]^2 \frac{(2m^*)^{1/2}}{F} E_k^{3/2} , \tag{14}$$

where the function F reads as

$$F = \ln(1+4k^2\lambda^2) - \frac{4k^2\lambda^2}{1+4k^2\lambda^2} .$$

The screening length λ was estimated from the Debye value $1/\lambda^2 = (e^2/\varepsilon_0\varepsilon_r)(dn/dE_F)$ in the presence of a degenerate electron density n.[10] To find the number of ionized impurities the Fermi level was determined numerically at temperature T from an equation which asserts electron conservation assuming that there are donors of one type only (P). The degree of ionization of the donors can then also be worked out. For the phosphorus concentration 10^{20} cm^{-3} the degree of ionization is $n/N_D = 0.16$ at 300 K and 0.50 at 900 K. The dielectric constant is $\varepsilon_r = 11.9$,[11] ε_0 is the permittivity of free space, and k is the positron wave vector. For the positron effective mass the same value $m^* = 1.6 m_e$ as above was adopted.

The diffusion coefficients D_{ii} in Si due to ionized-impurity scattering with $[{\rm P}] = 10^{20}$ cm^{-3} are plotted in Fig. 4. The lower solid curve in Fig. 4 has been obtained by combining the calculated scattering rates due to phonon processes [Eqs. (12) and (13)] with scattering rates due to interactions with ionized impurities [Eq. (14)]. Because of the approximations in the Brooks-Herring model (see below) the total mobility was taken simply as $\mu^{-1} = \Sigma(1/\mu_i)$. When the impurity concentration is of the order of 10^{20} cm^{-3} positron motion in Si is affected by ionized impurities at temperatures as high as 900 K. The experimental values for the positron diffusion coefficient in Si($[{\rm P}] = 10^{20}$ cm^{-3}) are in a qualitative agreement with this simple calculation. Any additional adjustable parameters were not needed to calculate the relaxation times due to impurity scattering.

At the doping concentration 10^{20} cm^{-3} the Brooks-Herring model for ionized-impurity scattering is not strictly valid. This is due to the approximations inherent in the theory, the Born approximation to calculate the scattering rates, and the single-potential approximation. We have also neglected positron-electron scattering. For electrons in p-type Si, the Brooks-Herring model predicts a mobility which is too large at 300 K if $N_A = 10^{20}$ cm^{-3}.[79,80] By analogy, the Brooks-Herring result is expected to overestimate the positron diffusion coefficients in n-type Si($[{\rm P}] = 10^{20}$ cm^{-3}).

B. Gallium arsenide

In this section we calculate the diffusion coefficients in GaAs due to combined longitudinal acoustic- and polar-optical-phonon scattering and compare the results with the experiment. Longitudinal acoustic-phonon scattering is treated in the deformation-potential formalism the same way as was done for Si. The momentum relaxation time is given by Eq. (12) and the parameters for GaAs are given in Table V. A band-structure calculation yields for the deformation-potential parameter $E_d = -5.83$ eV.[81]

The experimental results for the diffusion coefficient in semi-insulating GaAs do not follow the temperature dependence $T^{-1/2}$ expected from acoustic-phonon

TABLE V. Material parameters for GaAs. These values were used to calculate the positron diffusion coefficient due to acoustic-phonon and polar-optical-phonon interactions [Eq. (12) and Ref. 82]. $\varepsilon(0)$ and $\varepsilon(\infty)$ are the low- and high-frequency limits of the dielectric constant, respectively. For description of the other parameters, see the caption of Table IV.

E_d (eV)	c_L (N/m^2)	m^*	$\hbar\omega$ (meV)	$\varepsilon(0)$	$\varepsilon(\infty)$
-5.87[a]	14.1×10^{10}[b]	$1.3 m_e$	35.3[c]	12.85[c]	10.89[c]

[a]Puska (Ref. 81).

[b]The average was calculated as $c_L = c_{12} + 2c_{44} + \frac{3}{5}(c_{11} - c_{12} - 2c_{44})$ (Ref. 10). Data from Ref. 11.

[c]Reference 11.

scattering. In view of the present results, it is thus concluded that other scattering processes must be involved in GaAs in the temperature range $T \geq 300$.

The high-temperature electron mobility in GaAs is limited by polar-optical-phonon scattering,[82] and the same can be expected to hold for positrons. Polar-optical-phonon scattering is both inelastic and anisotropic, and a universal relaxation time cannot be defined. Therefore, we follow the calculation of Fletcher and Butcher which is an exact solution of the linearized Boltzmann equation based on its reduction to a coupled set of finite-difference equations.[82] This calculation yields the mobility which we relate to the diffusion coefficient via the Einstein relation. The necessary material parameters, the optical-phonon energy $\hbar\omega$, and the static and high-frequency dielectric constants $\varepsilon(0)$ and $\varepsilon(\infty)$ are listed in Table V.

The calculated positron diffusion coefficients in GaAs due to longitudinal acoustic- and polar-optical phonons are presented in Fig. 5. Using for the only adjustable parameter $m^*=1.3m_e$ there is a good agreement between the experiment and the theory in the temperature range 300 K $< T <$ 800 K. The present experimental data indicate that positron diffusion in GaAs is limited by longitudinal acoustic and polar-optical phonons.

We have explicitly calculated the positron diffusion coefficients in GaAs due to piezoelectric acoustic-phonon interaction in the relaxation-time approximation. The results are typically more than an order of magnitude higher than the experimental values and indicate that the effect to the total diffusion coefficient is small in the whole temperature range. The semi-insulating GaAs sample had intrinsic impurities in the level $10^{15}-10^{16}$ cm^{-3}. A calculation using the relaxation time of Eq. (14) shows that an ionized impurity concentration of 10^{16} cm^{-3} has no effect on positron diffusion in GaAs.

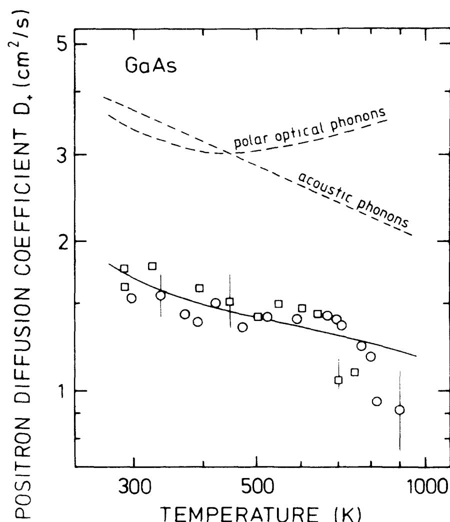

FIG. 5. Positron-lattice-scattering mechanisms in GaAs. The experimental data is reproduced from Fig. 2(b). The dashed curves are the calculated positron diffusion coefficients due to acoustic- and polar-optical-phonon scattering (see text and Table V). The solid curve is obtained by combining the contributions of the two phonon modes.

At temperatures higher than 700–800 K the experimental data indicates an unaccounted decrease in the diffusion coefficients. The values of D_+ at lower temperatures were reproduced after the measurements above 800 K. Positron trapping in the bulk is excluded as the parameter S_b showed no change at high temperatures. It does not seem plausible that the decrease in the experimental data could be due to the onset of nonpolar-optical-phonon scattering. Because of the relatively low optical-phonon energy of 35 meV, one would expect such effects to appear already at lower temperatures, and it does not account for the sharp decrease of D_+. The decrease may be due to dissociation of the GaAs surface at elevated temperatures which leads to changes in the electric charge at the surface[67] and possibly to an electric field which affects positron motion (cf. Sec. V).

C. Germanium

In Ge the same scattering mechanisms are expected to dominate positron diffusion as in Si. The longitudinal acoustic and first-order optical phonons were treated in the deformation-potential formalism the same way as was done for Si, with m^* and Ξ_1 as adjustable parameters and $E_d=-6.62$ eV (Ref. 8) [Eqs. (12) and (13)]. The line $D_+ \propto T^{-1/2}$ plotted through the data in Fig. 2(c) has been obtained by considering the acoustic phonons only and by using $m^*=1.6m_e$. The agreement between the data and the calculation is good for $T>500$ K. We have also considered both acoustic and optical phonons by taking for the optical deformation-potential parameter its value in Si $\Xi_1=11$ eV. By use of $m^*=1.45m_e$ a good agreement with the data was reached. As can be seen in Fig. 2(c), the experiment did not give a unique value for the 300-K diffusion coefficient in Ge. This makes the identification of the two-phonon processes difficult. However, both experimental values of D_+ at 300 K are close to the $T^{-1/2}$ dependence extrapolated from high temperatures. It is thus justified to conclude that acoustic-phonon scattering is the dominating scattering process of positrons in Ge from 300 to 970 K.

By inspection of Eqs. (12) and (14) it can be seen that the contribution of impurity scattering as compared to acoustic-phonon scattering decreases as the effective mass increases. Owing to the large positron effective mass, effects due to impurity scattering in Ge with an ionized impurity concentration 1.5×10^{17} cm^{-3} are not expected to be seen in positron diffusion results in contrast with electron mobilities. A calculation using the relaxation time of Eq. (14) for the ionized-impurity limited positron diffusion coefficient in the Ge([As]$=1.5\times10^{17}$ cm^{-3}) sample indicates that this impurity concentration is far too small to influence positron diffusion at 300 K. Since impurity scattering is not important and positron motion is not hindered by trapping (Sec. III B) or electric fields (Sec. V), the experimental result $D_+=0.84(9)$ cm^2/s should be a representative value of the lattice positron diffusion coefficient in Ge at 300 K. We thus conclude that the present experiment leaves some uncertainty about the 300-K value of the positron diffusion coefficient in Ge (0.8–2.1 cm^2/s).

VII. CONCLUSIONS

We have reported on a positron-beam study of Si, GaAs and Ge where positron diffusion coefficients were determined in the temperature range 130–1000 K. In Si the temperature dependence of the diffusion coefficient is $D_+ \propto T^{-1/2}$ from 130 to 500 K. By combining with the experimental results of Mäkinen *et al.*[37] the power law is observed to hold in Si from 30 to 500 K. The same temperature dependence was found for Ge at $T > 500$ K. In GaAs the diffusion coefficient shows only a weak temperature dependence at 300–800 K. In accordance with the recent studies, new parameters for the positron implantation profile have been adopted. The choice of parameters only affects the absolute values of the positron diffusion coefficients which in Si, GaAs, and Ge at 300 K were determined to be 2.3(2), 1.6(2), and 0.8–2.1 cm^2/s, respectively.

We have theoretically considered positron scattering from various long-wavelength longitudinal phonon modes. In Si and Ge positron scattering is dominated by interactions with acoustic phonons. In the lowest order, positron coupling to optical-phonon modes is forbidden by selection rules. However, we have demonstrated that in Si the agreement between the high-temperature data and the theory is greatly improved by inclusion of the first-order optical-phonon processes. We estimate the first-order optical deformation-potential parameter to be 11 eV. Similar first-order processes have been assumed, e.g., in Si to satisfactorily fit the experimental results of electron mobility. Such first-order processes are difficult to recognize with electrons or holes due to the complexity of their lattice interactions. In GaAs the data in the temperature range 300–800 K can be interpreted by including positron scattering from acoustic and polar-optical phonons with approximately equal scattering rates.

The effect of impurities was studied in a Si([P]$=10^{20}$ cm^{-3}) sample. A significant reduction in the positron diffusion coefficient was seen at 300–800 K. Positron scattering from ionized impurities gives a qualitatively correct description of the diffusion coefficients.

It was demonstrated that space-charge effects can have dramatic effects on positron motion near free semiconductor surfaces. Very high diffusion parameters were obtained from the free Ge surface near 300 K. Under flat-band conditions the diffusion parameters were much lower. The origin and consequences of the space-charge phenomena in Ge, Si, and GaAs were discussed.

A good agreement between the experiment and the calculations holds using theoretical acoustic deformation-potential parameters and positron effective masses of $m^* = 1.3-1.6 m_e$. These effective masses are in good agreement with other experimental and theoretical estimates. We are entitled to conclude that weak coupling of positrons with the lattice gives a good description of positron motion in Si, GaAs and Ge up to 1000 K.

ACKNOWLEDGMENTS

The authors thank S. Palko for experimental assistance in the preparation and characterization of Schottky diodes. J. Martikainen is acknowledged for the Monte Carlo simulations and Z. Kantor for the electric-field calculations. We are indebted to M. Puska for many useful discussions and the band-structure calculation of the theoretical coupling constant in GaAs, and to R. Nieminen for critical reading of the manuscript. We are grateful to P. Corvo, A. Freundlich, E. Haller, D. Mathiot, E. Molva, and F. Vanoni for providing the samples and to J. Vaari for the XPS analyses. The work of E.S. has been partially supported by the Jenny and Antti Wihuri Foundation.

[1]S. M. Sze, *Physics of Semiconductors Devices,* 2nd ed. (Wiley, New York, 1981).

[2]G. Ottaviani, L. Reggiani, C. Canali, F. Nava, and A. Alberigi-Quaranta, Phys. Rev. B **12**, 3318 (1975).

[3]C. Canali, C. Jacoboni, F. Nava, G. Ottaviani, and A. Alberigi-Quaranta, Phys. Rev. B **12**, 2265 (1975).

[4]L. Reggiani, F. Canali, F. Nava, and G. Ottaviani, Phys. Rev. B **16**, 2781 (1977).

[5]C. Jacoboni, F. Nava, C. Canali, and G. Ottaviani, Phys. Rev. B **24**, 1014 (1981).

[6]We are aware of studies of carrier mobilites at high temperatures only in GaAs. See K. H. Nichols, C. M. L. Yee, and C. M. Wolfe, Solid State Electron. **23**, 109 (1980).

[7]T. Hyodo, T. McMullen, and A. T. Stewart, Phys. Rev. B **33**, 3050 (1986).

[8]O. V. Boev, M. J. Puska, and R. M. Nieminen, Phys. Rev. B **36**, 7786 (1987).

[9]P. N. Butcher, in *Crystalline Semiconducting Materials and Devices,* edited by P. N. Butcher, N. H. March, and M. P. Tosi (Plenum, New York, 1986).

[10]B. K. Ridley, *Quantum Processes in Semiconductors,* 2nd ed. (Clarendon, Oxford, 1988).

[11]*Semiconductors: Group IV Elements and III-V Compounds (Data in Science and Technology),* edited by O. Madelung (Springer, Berlin, 1991).

[12]*Positrons in Solids,* edited by P. Hautojärvi, Topics in Current Physics Vol. 12 (Springer, Heidelberg, 1979).

[13]J. Mäkinen, E. Punkka, A. Vehanen, P. Hautojärvi, J. Keinonen, M. Hautala, and E. Rauhala, J. Appl. Phys. **67**, 990 (1990).

[14]J. Keinonen, M. Hautala, E. Rauhala, V. Karttunen, A. Kuronen, J. Räisänen, J. Lahtinen, A. Vehanen, E. Punkka, and P. Hautojärvi, Phys. Rev. B **37**, 8269 (1988).

[15]K. Saarinen, P. Hautojärvi, J. Keinonen, E. Rauhala, J. Räisänen, and C. Corbel, Phys. Rev. B **43**, 4249 (1991).

[16]T. E. Jackman, G. C. Aers, M. W. Denhoff, and P. J. Schultz, Appl. Phys. A **49**, 335 (1989).

[17]B. Nielsen, K. G. Lynn, T. C. Leung, B. F. Cordts, and S. Seraphin, Phys. Rev. B **44**, 1812 (1991).

[18]A. Uenodo, L. Wei, Y. Tabuki, H. Kondo, S. Tanigawa, J. Sugiara, M. Ogasawara, C. Dosho, M. Tamura, K. Wada, and H. Nakanishi, in *Proceedings of the IX Conference on Positron Annihilation,* Szombathely, Hungary, 1991 (Trans Tech., Aedermannsdorf, Switzerland, 1992).

[19]P. J. Schultz, E. Tandberg, K. G. Lynn, B. Nielsen, T. E. Jackman, M. W. Denhoff, and G. C. Aers, Phys. Rev. Lett. **61**,

187 (1988).

[20]P. G. Coleman, N. B. Chilton, and J. A. Baker, J. Phys. Condens. Matter **2**, 9355 (1990).

[21]B. Nielsen, K. G. Lynn, D. O. Welch, T. C. Leung, and G. W. Rubloff, Phys. Rev. B **40**, 1434 (1989).

[22]J. A. Baker, and P. B. Coleman, J. Phys. Condens. Matter **1**, SB39 (1989).

[23]Y. Tabuki, L. Wei, S. Tanigawa, K. Hinode, N. Kobayashi, T. Onai, and N. Owada, in *Proceedings of the IX Conference on Positron Annihilation* (Ref. 18).

[24]P. Asoka-Kumar, K. G. Lynn, T. C. Leung, B. Nielsen, G. W. Rubloff, and Z. A. Weinberg, Phys. Rev. B **44**, 5885 (1991).

[25]K. G. Lynn and B. T. A. McKee, Appl. Phys. **19**, 247 (1979).

[26]A. P. Mills, Jr. and C. A. Murray, Appl. Phys. **21**, 323 (1980).

[27]C. D. Beling, R. I. Simpson, M. Charlton, F. M. Jacobsen, T. C. Griffith, P. Moriatry, and S. Fung, Appl. Phys. A **42**, 111 (1987).

[28]A. P. Mills, Jr. and L. Pfeiffer, Phys. Rev. Lett. **36**, 1389 (1976).

[29]A. P. Mills, Jr. and L. Pfeiffer, Phys. Lett. **63A**, 118 (1977).

[30]C. D. Beling (private communication); H. L. Au, C. C. Ling, T. C. Lee, C. D. Beling, and S. Fung, in *Proceedings of the IX Conference on Positron Annihilation* (Ref. 18). In the original paper the authors report the positron mobility 30 $cm^2/V\,s$ in GaAs at 300 K but an improved measurement at 300 K gives the mobility 80 $cm^2/V\,s$.

[31]W. Brandt and R. Paulin, Phys. Rev. B **15**, 2511 (1977).

[32]R. I. Simpson, M. G. Stewart, C. D. Beling, and M. Charlton, J. Phys. Condens. Matter **1**, 7251 (1989).

[33]A. P. Mills, Jr., Phys. Rev. Lett. **41**, 1828 (1978).

[34]B. Nielsen, K. G. Lynn, A. Vehanen, and P. J. Schultz, Phys. Rev. B **32**, 2296 (1985).

[35]H. H. Jorch, K. G. Lynn, and I. K. MacKenzie, Phys. Rev. Lett. **47**, 362 (1981).

[36]H. H. Jorch, K. G. Lynn, and T. McMullen, Phys. Rev. B **30**, 93 (1984).

[37]J. Mäkinen, C. Corbel, P. Hautojärvi, and D. Mathiot, Phys. Rev. B **43**, 12 114 (1991).

[38]J. Mäkinen, C. Corbel, P. Hautojärvi, A. Vehanen, and D. Mathiot, Phys. Rev. B **42**, 1750 (1990).

[39]K. Saarinen, P. Hautojärvi, A. Vehanen, R. Krause, and G. Dlubek, Phys. Rev. B **39**, 5287 (1989).

[40]P. C. Rice-Evans, D. L. Smith, H. E. Evans, and G. A. Gledhill, in *Positron Beams for Solids and Surfaces,* edited by P. J. Schultz, G. R. Massoumi, and P. J. Simpson, AIP Conference Proceedings No. 218 (American Institute of Physics, New York, 1991), p. 147.

[41]E. Soininen, H. Huomo, P. A. Huttunen, J. Mäkinen, A. Vehanen, and P. Hautojärvi, Phys. Rev. B **41**, 6627 (1990).

[42]P. J. Schultz and K. G. Lynn, Rev. Mod. Phys. **60**, 701 (1988).

[43]H. Huomo, E. Soininen, and A. Vehanen, Appl. Phys. A, **49**, 647 (1989).

[44]W. Brandt, in *Positron Solid State Physics,* edited by W. Brandt (North-Holland, Amsterdam, 1983), p. 1.

[45]T. McMullen, in *Positron Annihilation,* edited by P. C. Jain, R. M. Singru, and K. P. Gopinathan (World Scientific, Singapore, 1985), p. 657.

[46]S. Valkealahti and R. M. Nieminen, Appl. Phys. A **35**, 51 (1984).

[47]R. M. Nieminen and J. Oliva, Phys. Rev. B **22**, 2226 (1980).

[48]J. Lahtinen, A. Vehanen, H. Huomo, J. Mäkinen, P. Huttunen, K. Rytsölä, M. Bentzon, and P. Hautojärvi, Nucl. Instrum. Methods **17**, 73 (1986).

[49]An almost flat $S(E)$ curve was observed in GaAs([Zn] $=10^{19}$ cm^{-3}).

[50]C. Corbel, M. Stucky, P. Hautojärvi, K. Saarinen, and P. Moser, Phys. Rev. B **38**, 8192 (1988).

[51]K. Saarinen (private communication). The lifetimes in Si and Si([P] $=10^{20}$ cm^{-3}) were measured in the same wafers as in this work, in the temperature range 20–500 K.

[52]P. Lanki (unpublished). The lifetime measurements in semi-insulating GaAs were performed in a temperature range 300–600 K.

[53]R. Würschum, W. Bauer, K. Maier, J. Major, A. Seeger, H. Stoll, H.-D. Carstanjen, W. Decker, J. Diehl, and H.-E. Schaefer, in *Positron Annihilation,* edited by L. Dorikens-Vanpraet, M. Dorikens, and D. Segers (World Scientific, Singapore, 1989), p. 671.

[54]T. Throwe, T. C. Leung, B. Nielsen, H. Huomo, and K. G. Lynn, Phys. Rev. B **40**, 12037.

[55]A. Vehanen, K. Saarinen, P. Hautojärvi, and H. Huomo, Phys. Rev. B **35**, 4606 (1987).

[56]J. A. Baker, N. B. Chilton, K. O. Jensen, A. B. Walker, and P. G. Coleman, J. Phys. Condens. Matter **3**, 4109 (1991).

[57]J. A. Baker, N. B. Chilton, and P. G. Coleman, Appl. Phys. Lett. **59**, 164 (1991).

[58]J. A. Baker, N. B. Chilton, K. O. Jensen, A. B. Walker, and P. G. Coleman, Appl. Phys. Lett. **59**, 2962 (1991).

[59]G. R. Massoumi, N. Hozhabri, W. N. Lennart, and P. J. Schultz, Phys. Rev. B **44**, 3486 (1991).

[60]H. Huomo, A. Vehanen, M. D. Bentzon, and P. Hautojärvi, Phys. Rev. B **35**, 8252 (1987).

[61]R. H. Howell, I. J. Rosenberg, and M. J. Fluss, Phys. Rev. B **34**, 3069 (1986).

[62]B. Nielsen, K. G. Lynn, and Y.-C. Chen, Phys. Rev. Lett. **57**, 1789 (1986).

[63]P. Asoka-Kumar and K. G. Lynn, Appl. Phys. Lett. **57**, 1634 (1990).

[64]E. H. Nicollian and J. R. Brews, *MOS (Metal Oxide Semiconductor) Physics and Technology* (Wiley, New York, 1982).

[65]B. Nielsen, K. G. Lynn, D. O. Welch, T. C. Leung, and G. W. Rubloff, Phys. Rev. B **40** 1434 (1989).

[66]P. M. Dryburgh, in *MOS Devices: Design and Manufacture,* edited by A. D. Milne (Edinburgh University Press, Edinburgh, 1982), p. 61.

[67]F. Proix, A. Akremi, and Z. T. Zhong, J. Phys. C **16**, 5499 (1983).

[68]E. Soininen, A. Schwab, and K. G. Lynn, Phys. Rev. B **43**, 10051 (1991).

[69]R. B. Darling, Phys. Rev. B **43**, 4071 (1991).

[70]A. Many, Y. Goldstein, and N. B. Grover, *Semiconductor Surfaces* (North-Holland, Amsterdam, 1965).

[71]F. G. Allen and G. W. Gobeli, Phys. Rev. **127**, 150 (1962).

[72]M. Schulz, Surf. Sci. **132**, 422 (1983).

[73]W. E. Spicer, I. Lindau, P. R. Skeath, and C. Y. Su, J. Vac. Sci. Technol. **17**, 1019 (1980); N. Newman, W. E. Spicer, T. Kendelewicz, and I. Landau, *ibid.* B **4**, 931 (1986).

[74]A. Thanailakis and D. C. Northrop, Solid State Electron. **16**, 1383 (1973).

[75]C. Pennetta, Solid State Commun. **77**, 159 (1991).

[76]R. Kubo, J. Phys. Soc. Jpn. **12**, 570 (1958).

[77]G. Ghibaudo, Phys. Status Solidi B **153**, K155 (1989).

[78]D. K. Ferry, Phys. Rev. B **14**, 1605 (1975).

[79]L. E. Kay and T.-W. Tang, J. Appl. Phys. **70** 1475 (1991).

[80]M. V. Fischetti, Phys. Rev. B **44**, 5527 (1991).

[81]M. Puska (private communication).

[82]K. Fletcher and P. N. Butcher, J. Phys. C **5**, 212 (1972).